J|A|C|S COMMUNICATIONS

Published on Web 04/28/2010

High-Performance Silicon Nanohole Solar Cells

Kui-Qing Peng,*,† Xin Wang,† Li Li,† Xiao-Ling Wu,† and Shuit-Tong Lee*,‡

Department of Physics and College of Nuclear Science and Technology, Beijing Normal University, Beijing 100875, China, and Center of Super-Diamond and Advanced Films (COSDAF) and Department of Physics and Materials Science, City University of Hong Kong, Hong Kong SAR, China

Received December 7, 2009; E-mail: kq_peng@bnu.edu.cn; apannale@cityu.edu.hk

Photovoltaic (PV) solar energy conversion represents a promising approach to green, renewable energy. Despite its advantages and continuing advances, PV technology remains non-cost-competitive against traditional fossil fuels and thus has not yet been mass-deployed. Recent research has focused on developing new PV systems that incorporate optically active nanostructures such as nanoparticles,[1] quantum dots,[2] nanotubes,[3] nanorods,[4,5] and nanowires,[6−19] which offer substantial potential for new device structures. Functional PV devices based on conformal radial p−n junction nanowires (alos called coaxial core/shell nanowires) are of particular interest as an optimal way to decouple light absorption from minority carrier collection.[8−16] Tian and co-workers have reported a single coaxial silicon nanowire (SiNW) solar cell with a short-circuit current density (J_{sc}) of 23.9 mA/cm^2 and a power conversion efficiency of 3.4% under 1 sun AM1.5G illumination.[10] Most of the current PV research on nanowires has focused on arrays of nanowires with solid-state radial p−n junctions.[12−16] For example, scalable SiNW-based solar cells with radial p−n heterojunctions have been fabricated with vapor−liquid−solid grown[12] and electrolessly etched SiNW arrays.[13] Unfortunately, all of those attempts thus far have yielded unsatisfactory results. The poor performance is predominantly attributed to large shunting across the cells and excessive surface or junction recombination losses. More recently, Garnet and Yang reported SiNW solar cells with an efficiency above 5% and short-circuit photocurrents higher than those of planar control samples.[20] In this work, we report the fabrication of a novel Si nanohole solar cell incorporating radial p−n junctions via thermal phosphorus dopant diffusion. Such a nanohole geometry exhibits superior mechanical robustness in comparison with free-standing nanowire counterparts, which are fragile and easily cracked. Moreover, the nanohole array structures display superior optical absorption ability resulting from effective optical coupling between the nanohole array and the incident light as well as a large density of waveguide modes.[21]

The wafer-scale ordered Si nanohole array was fabricated by the combination of deep ultraviolet lithography (UVL) and metal-assisted Si etching in aqueous oxidizing hydrofluoric acid (HF).[22] Figure S1 in the Supporting Information illustrates the fabrication process. Figure 1 shows typical scanning electron microscopy (SEM) images of Si nanoholes produced from a p-type Si(100) wafer with a resistivity of 8−12 Ω cm in an aqueous solution of HF and H_2O_2. The concentrations of HF and H_2O_2 were 10 and 0.6%, respectively. The pore diameters and wall thicknesses were defined by a chromium mask and deep UVL, while the nanohole depths were adjusted by the etching time. Figure 1a is a top-view SEM image of the ordered, shallow, flat-bottomed pits in Si formed during the initial etching stage, where a silver film can be clearly seen. These shallow pits would grow into deep holes upon prolonged immersion in the oxidizing HF solution. Figure 1b,c shows top-view SEM images of large-area silicon nanoholes. They show that the holes are regularly distributed on the Si surface and that the thicknesses of the hole walls are 280 and 880 nm for the first-neighbor and second-neighbor holes, respectively. Figure 1d is a SEM image of a cross section of the holes, showing that the channels are cylindrical and vertical with respect to the wafer surface.

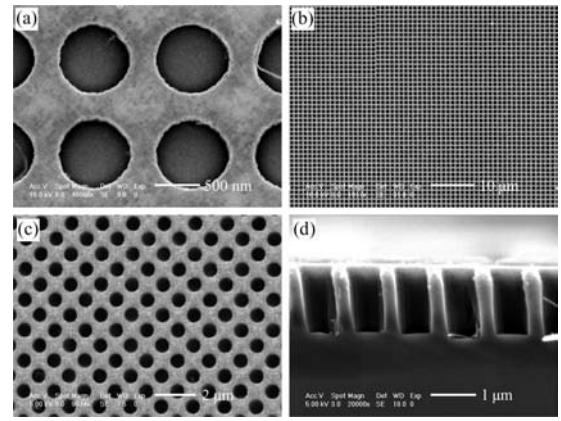

Figure 1. SEM images of silicon nanoholes produced in an 8−12 Ω cm p-Si(100) wafer. (a) Top-view SEM image of ordered, shallow, flat-bottomed pits in Si formed during the initial etching stage. Silver is seen at the bottom of these pits. (b, c) Top-view SEM images of ordered silicon nanoholes with large depths after prolonged immersion in HF and H_2O_2 solution. (d) Cross-sectional view of silicon nanoholes; the hole channels are cylindrical and vertical with respect to the Si surface.

Figure 2 illustrates the fabrication process of the radial p−n junctions in our Si nanohole solar cell. The Si nanohole sample was first washed with excess deionized water, and silver was removed with concentrated nitric acid. RCA cleaning was carried out to further eliminate the residual metal and organic species, after which Si oxide was removed with a buffered HF solution. Next, a continuous thin n^+ layer ∼150−200 nm in thickness was formed on the exposed external and internal surfaces of the Si nanoholes via phosphorus dopant diffusion at 910 °C for 20 min using a liquid $POCl_3$ source. After removal of the phosphorosilicate glass layer in a diluted HF solution, an aluminum layer was evaporated onto the rear surface and treated at 980 °C to remove the rear parasitic p−n junction and concurrently form a back-surface field on the back side of the wafer. Afterward, a 200 nm aluminum layer and Ti/Pd/Ag grid contacts were deposited onto the rear and front sides of the Si nanoholes, respectively. Good Ohmic contacts were achieved by annealing at 380 °C. A prototype Si nanohole solar cell was created after removal of the circumferential parasitic p−n junction, as shown in Figure S2. Such a nanohole solar cell offers several distinct advantages associated with its unique geometry. First, it consists of well-separated functional radial p−n junctions,

† Beijing Normal University.
‡ City University of Hong Kong.

10.1021/ja910082y

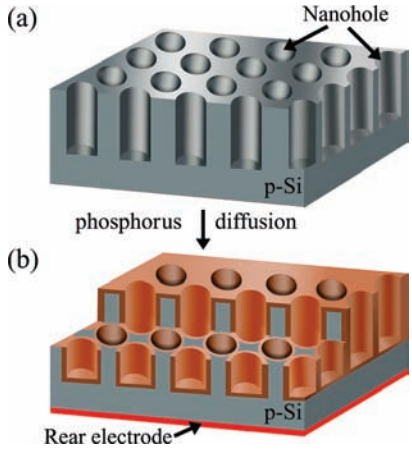

Figure 2. Sectional elevation of the process of fabricating the Si nanohole solar cell with radial p−n junctions via thermal phosphorus dopant diffusion. The n^+ layer is shown in purple bronze, the p-Si substrate in gray, and the rear electrode in red; the front Ti/Pd/Ag grid electrode is not shown here.

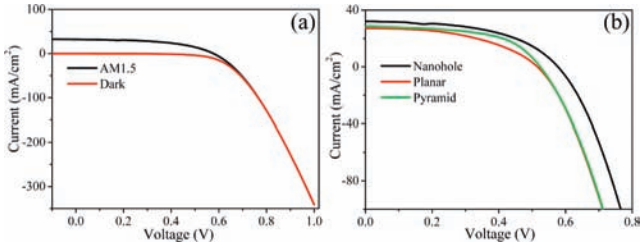

Figure 3. (a) $I-V$ curves for Si nanohole solar cells in the dark and under AM1.5 illumination. (b) $I-V$ curves for solar cells with different geometries fabricated under identical conditions.

because the thin walls between the first-neighbor pores are fully depleted, while the thick walls between the second-neighbor pores remain quasi-neutral for efficient channeling of holes to the p-type substrate (Figure 2b). Such vertically configured p−n junctions enable photogenerated minority carriers to travel only short distances to junctions for efficient carrier collection. Second, our solar cell made of radial p−n junction arrays with a common n^+ layer forming an interconnecting porous structure provides superior mechanical robustness, far better than in the fragile structure of a free-standing nanowire radial p−n junction solar cell. Third, the homojunctions via thermal diffusion facilitate migration of photo-excited minority carriers across interfaces and reduce interfacial recombination. An additional advantage is that the interconnecting nanohole geometry would ease electrode fabrication while avoiding breakdown of the radial p−n junctions. This feature is particularly important since it circumvents the fragility problem of the free-standing nanowire geometry in electrode fabrication, which has seriously impeded applications.

The PV properties of the Si nanohole solar cells were investigated under an ORIEL solar simulator with 1 sun AM1.5G illumination. Figure 3a shows the output characteristics of a typical Si nanohole solar cell with hole depths of ~2 μm. The dark current−voltage ($I-V$) curve of the device shows $I-V$ characteristics similar to those of an ideal diode. Under illumination, the device exhibits an open-circuit voltage (V_{oc}) of 566.6 mV, a J_{sc} of 32.2 mA/cm^2, and a fill factor of 0.522, giving an energy conversion efficiency (η) of 9.51%, which is much higher than the values reported for SiNW radial p−n junction solar cells. Figure 3b shows the output characteristics of differently shaped solar cells fabricated under identical conditions. The Si nanohole device shows a substantively larger J_{sc} and efficiency than its counterparts based on planar Si, pyramid-textured Si, and SiNWs, demonstrating that nanohole arrays are better than other geometrical textures in PV performance improvement and thus represent a meritorious and viable approach for efficient solar PVs. This observation is supported by recently theoretical results.[21] According to the mask used for the front electrode, 20% of the front surface area of the nanohole device was covered by the front contact; thus, the effective J_{sc} for the nanohole solar cell is 40 mA/cm^2 after exclusion of the front contact area. Figure S3 shows the external quantum efficiency (EQE) for the nanohole solar cell, which exhibits a spectrally broad EQE response. We expect device optimization (e.g., improved coupling of light into the device), surface passivation, and better contacts to further enhance the performance of the Si nanohole solar cell.

In summary, we have demonstrated the fabrication of a silicon nanohole solar cell consisting of three-dimensional radial p−n junctions. Under 1 sun AM1.5G illumination, the nanohole solar cell exhibited a V_{oc} of 566.6 mV, a J_{sc} of 32.2 mA/cm^2, and a power conversion efficiency of 9.51%, which are superior to those of its counterparts based on SiNWs, planar Si, and pyramid-textured Si. The nanohole array geometry holds great potential for cost-efficient PV solar energy conversion.

Acknowledgment. This work was supported by the National 973 Project of China (Grant 2006CB933000), the NSFC (Grant 50702010), National Excellent Doctoral Dissertations of China (Grant 200743), Beijing Natural Science Foundation (Grant 2082013), NCET-08-0060, Beijing Nova Program 2008B24, a Research Grants Council of Hong Kong SAR−CRF Grant (Grant CityU5/CRF/08), and the Joint Research Project of RGC and NSFC (Grant N_CityU108/08). Dr. Y. Xu is thanked for her contributions.

Supporting Information Available: Experimental details of fabrication of silicon nanohole arrays and solar cells. This material is available free of charge via the Internet at http://pubs.acs.org.

References

(1) O'Regan, B.; Grätzel, M. *Nature* **1991**, *353*, 737.
(2) Schaller, R. D.; Agranovich, V. M.; Klimov, V. I. *Nat. Phys.* **2005**, *1*, 189.
(3) Gabor, N. M.; Zhong, Z.; Bosnick, K.; Park, J.; McEuen, P. L. *Science* **2009**, *325*, 1367.
(4) Huynh, W. U.; Dittmer, J. J.; Alivisatos, A. P. *Science* **2002**, *295*, 2425.
(5) Law, M.; Greene, L. E.; Johnson, J. C.; Saykally, R.; Yang, P. D. *Nat. Mater.* **2005**, *4*, 455.
(6) Peng, K.; Xu, Y.; Wu, Y.; Yan, Y. J.; Lee, S. T.; Zhu, J. *Small* **2005**, *1*, 1062.
(7) Leschkies, K. S.; Divakar, R.; Basu, J.; Enache-Pommer, E.; Boercker, J. E.; Carter, C. B.; Kortshagen, U. R.; Norris, D. J.; Aydil, E. S. *Nano Lett.* **2007**, *7*, 1793.
(8) Tian, B. Z.; Zheng, X. L.; Kempa, T. J.; Fang, Y.; Yu, N. F.; Yu, G. H.; Huang, J. L.; Lieber, C. M. *Nature* **2007**, *449*, 885.
(9) Kayes, B. M.; Atwater, H. A.; Lewis, N. S. *J. Appl. Phys.* **2005**, *97*, 114302.
(10) Tian, B.; Kempa, T. J.; Lieber, C. M. *Chem. Soc. Rev.* **2009**, *38*, 16.
(11) Dong, Y.; Tian, B.; Kempa, T.; Lieber, C. M. *Nano Lett.* **2009**, *9*, 2183.
(12) Tsakalakos, L.; Balch, J.; Fronheiser, J.; Korevaar, B. A.; Sulima, O.; Rand, J. *Appl. Phys. Lett.* **2007**, *91*, 233117.
(13) Garnett, E. C.; Yang, P. D. *J. Am. Chem. Soc.* **2008**, *130*, 9224.
(14) Czaban, J. A.; Thompson, D. A.; LaPierre, R. R. *Nano Lett.* **2009**, *9*, 148.
(15) Yuhas, B.; Yang, P. D. *J. Am. Chem. Soc.* **2009**, *131*, 3756.
(16) Fan, Z.; Razavi, H.; Do, J.; Moriwaki, A.; Ergen, O.; Chueh, Y.; Leu, P.; Hol, J.; Takahashi, T.; Reichertz, L.; Neale, S.; Yu, K.; Wu, M.; Ager, J.; Javey, A. *Nat. Mater.* **2009**, *8*, 648.
(17) Peng, K. Q.; Wang, X.; Wu, X. L.; Lee, S. T. *Nano Lett.* **2009**, *9*, 3704.
(18) Muskens, O. L.; Rivas, J. G.; Algra, R. E.; Bakkers, E. P. A. M.; Lagendijk, A. *Nano Lett.* **2008**, *8*, 2638.
(19) Sivakov, V.; Andra, G.; Gawlik, A.; Berger, A.; Plentz, J.; Falk, F.; Christiansen, S. H. *Nano Lett.* **2009**, *9*, 1549.
(20) Garnet, E.; Yang, P. D. *Nano Lett.* **2010**, *10*, 1082.
(21) Han, S. E.; Chen, G. *Nano Lett.* **2010**, *10*, 1012.
(22) (a) Peng, K. Q.; Lu, A. J.; Zhang, R. Q.; Lee, S. T. *Adv. Funct. Mater.* **2008**, *18*, 3026. (b) Peng, K. Q.; Wang, X.; Wu, X. L.; Lee, S. T. *Appl. Phys. Lett.* **2009**, *95*, 143119.

JA910082Y